

Intermittency of surface layer wind velocity series in the mesoscale range

Jean-François Muzy*

*CNRS UMR 6134, Université de Corse,
Quartier Grossetti, 20250, Corte, France*

Rachel Baïle[†] and Philippe Poggi[‡]

CNRS UMR 6134, Université de Corse, Vignola, 20200, Ajaccio, France

(Dated: December 12, 2009)

Abstract

We study various time series of surface layer wind velocity at different locations and provide evidences for the intermittent nature of the wind fluctuations in mesoscale range. By means of the magnitude covariance analysis, which is shown to be a more efficient tool to study intermittency than classical scaling analysis, we find that all wind series exhibit similar features than those observed for laboratory turbulence. Our findings suggest the existence of a "universal" cascade mechanism associated with the energy transfer between synoptic motions and turbulent microscales in the atmospheric boundary layer.

PACS numbers: 92.60.Aa, 92.60.Fm, 47.27.eb, 47.53.+n

*Electronic address: muzy@univ-corse.fr

[†]Electronic address: baile@univ-corse.fr

[‡]Electronic address: poggi@univ-corse.fr

I. INTRODUCTION

Atmospheric surface layer motions are a source of many challenging problems. The issue of designing a faithful statistical model of spatio-temporal wind speed fluctuations has been addressed in various fields like boundary layer turbulence phenomenology, meteorology, wind power control and prediction or climatology. From turbulent gusts to hurricanes, breezes to geostrophic wind, the wind process is characterized by a wide range of spatio-temporal scales and all the above mentioned disciplines mainly focus on a specific subrange of scales. The modeling of wind speed behavior in the mesoscale range is of great interest for example in wind power generation or in order to control pollutant dispersion. In this range of scales extending from few minutes to few days ($\sim 1\text{-}1000$ km), the properties of wind velocities are less known than in the range of planetary motions (synoptic scales) or turbulent motions (microscales) [1, 2]. From a physical point of view, because of the importance of boundary conditions, the heterogeneous and non-stationary nature of the processes involved, it is well admitted that mesoscale wind regimes strongly depend upon various factors like atmospheric conditions, the nature of the terrain and may involve periodic variations (caused by diurnal temperature variations). Unlike microscale Kolmogorov homogeneous turbulence, mesoscale fluctuations are therefore not expected to possess any degree of universality [3]. However, during past few years, some papers have been devoted to the analysis of scaling laws and intermittency features at large scales in many geophysical signals like temperature, rainfall or wind speeds [4, 5, 6]. In Ref. [3], the authors showed that surface layer wind velocities recorded at low frequency using a cup anemometer display multiscaling properties very much like in the high frequency turbulent regime. Moreover, they claimed that random cascade models could be pertinent to reproduce the observed intermittent fluctuations. Along the same line, in [7], a Multifractal Detrended Analysis was performed on four different hourly wind speed records and revealed some multiscaling properties of the series. Even if these studies did not go beyond simple scaling exponent estimation and did not consider problems related to the statistical significance of the obtained results, they had the merit to address questions about the possible intermittent nature of wind variations in the mesoscale range. As reviewed below, one of the consequences of multiscaling and intermittency is that small scales fluctuations are strongly non Gaussian and characterized by "bursty" behavior. In Refs. [8, 9], such features have been precisely observed on wind variations statistics at largest

microscales (or at smallest mesoscales) and have been shown to be related to a “fluctuating” log-normal turbulent intensity.

In this paper we suggest that this “fluctuating turbulent intensity” results from a random cascading process initiated at a time scale of few days. Our aim is to show that, in some sense, “turbulent” cascade models are likely to be pertinent at larger scales, in the so-called mesoscale regime. As compared to the previously cited papers, our analysis relies upon the use of magnitude (i.e. logarithms of velocity increments amplitudes) correlation functions. From a mathematical point of view, long-range correlated magnitudes have been shown to be at the heart of the construction of continuous cascade processes [10, 11]. For a practical point of view, magnitude covariance possesses interesting properties as far as statistical estimation problems are concerned [12, 13, 14]. We show that these correlation functions can be reliably estimated and are very similar to those associated with longitudinal velocity time series of laboratory turbulent experiments. Moreover we observe some universal features among the various analyzed series.

The paper is organized as follows: in section II, we make a brief review of intermittency and the related notion of random cascade models. We emphasize on the interest of studying magnitude correlations and discuss its relationship with multiscaling properties. We then compare, on an empirical ground, the relative performances of intermittency estimators relying upon scaling and magnitude covariance. This section ends with a review of a recent work of B. Castaing that has shown how intermittency in Lagrangian and Eulerian frames is “observed” on time series recorded at a fixed spatial position. Our main experimental results are then presented in section III. After a rapid description of various wind data we have studied, we show that wind surface layer variations in mesoscale range have intermittent properties and possess “universal” magnitude covariance similar to laboratory turbulent fluctuations. Discussions and prospects are reported in section IV.

II. INTERMITTENCY: FROM MULTISCALING TO MAGNITUDE CORRELATIONS

A. Multiscaling and intermittency

Small scale intermittency is one of the most challenging problems in contemporary turbulence research. It is generally associated with two distinctive features: the first one is that at small scales the probability density functions (pdf) of velocity variations are strongly leptokurtic (with "stretched exponential" tails) while they are almost gaussian at larger scales. The second one is that the so-called structure functions display multiscaling properties. As we shall see, these two properties are in fact equivalent within the multiplicative cascade picture. Let us make a brief overview of these notions.

We denote $X(t)$ a continuous process (for instance the time variations of a velocity field component at a fixed location) and let $\delta_\tau X(t)$ be its increments over a scale τ : $\delta_\tau X(t) = X(t + \tau) - X(t)$. One usually defines the order q structure function of X as

$$S_q(\tau) = \int |\delta_\tau X(u)|^q du \quad (1)$$

and the $\zeta(q)$ spectrum as the scaling exponent of $S_q(\tau)$:

$$S_q(\tau) \underset{\tau \rightarrow 0}{\sim} \tau^{\zeta(q)} \quad (2)$$

If the function $\zeta(q)$ is non-linear one says that $X(t)$ is a multifractal process or an intermittent process. In that case, as shown e.g. in [15], $\zeta(q)$ is necessarily a concave function and the previous scaling holds in the range of small τ ; $\tau \rightarrow 0$ means precisely $\tau \ll T$ where T is a coarse scale called the integral scale in turbulence (in general associated with the injection scale). The intermittency coefficient is a positive number that quantifies the non-linearity of $\zeta(q)$ and can be defined ¹ as, e.g.,

$$\lambda^2 = -\zeta''(0) \quad (3)$$

The most common example of non linear $\zeta(q)$ function is the so-called *log-normal* spectrum which is a simple parabola:

$$\zeta(q) = \alpha q - \frac{\lambda^2}{2} q^2 \quad (4)$$

¹ Notice that one can find different definitions of the "intermittency coefficient" or the "intermittency exponent" in the literature (see [16] for example). However within the log-normal cascade model discussed below they are all equivalent.

In that case λ^2 corresponds to the constant curvature of $\zeta(q)$.

In order to estimate the multiscaling properties and/or the intermittency coefficient, one can directly estimate partition functions from the data and obtain the exponent $\zeta(q)$ from a least square fit of $S_q(\tau)$ in log-log representation. However this method suffers from various drawbacks. First, from a fundamental point of view, one has to distinguish temporal (or spatial) averages from ensemble averages. For instance, in the case of a log-normal multifractal, rigorously speaking, only the “ensemble” average $\langle |\delta_\tau X(u)|^q \rangle$ behaves as a power law with an exponent $\zeta(q)$ as given by Eq. (4). The temporal or spatial average has an exponent spectrum $\zeta(q)$ that becomes linear above some value of q and is no longer parabolic [17]. In order to estimate $\zeta(q)$ from moment scaling over a wide range of q one has to use the so-called “mixed” asymptotic framework [18]. But the main problem remains that high order moment estimates require very large sample size. Moreover the scaling behavior can also be altered by finite size effects, discreteness and non stationarity effects like periodic perturbations or periodic modulations of the data (see below). A more reliable method first introduced in [12] (see also [19]) relies upon the so-called magnitude cumulant analysis. It simply consists in focusing on the scaling behavior of partition functions around $q = 0$. According to this approach, the structure function is written as:

$$S_q(\tau) = \exp \left(\sum_{k=1}^{\infty} C_k(\tau) \frac{q^k}{k!} \right) \quad (5)$$

where $C_k(\tau)$ is the k -th cumulant associated with the random variable $\omega_\tau(u) = \ln(|\delta_\tau X(u)|)$. The logarithm of the increment will henceforth be referred to as the *magnitude* of velocity increments. Note that C_1 is simply the mean value of ω while C_2 is its variance. Thanks to the scaling relationship (2), one deduces that all cumulants behave as:

$$C_k(\tau) = c_k \ln(\tau) + r_k \quad (6)$$

where the constants $\{r_k\}$ account for both the integral scale and the prefactors in the scaling relationship (2). The function $\zeta(q)$ can therefore be expressed in terms of a cumulant expansion:

$$\zeta(q) = \sum_k c_k \frac{q^k}{k!} \quad (7)$$

In particular one sees that the intermittency coefficient is directly involved in the behavior of the magnitude variance as:

$$C_2(\tau) = -\lambda^2 \ln(\tau) + r_2 . \quad (8)$$

Eq. (8) has been successfully used to estimate the intermittency coefficient of longitudinal velocity fields in 3D fully developed regime under various experimental conditions. A common value close to $\lambda^2 \simeq 0.025$ has been obtained. It is remarkable that this intermittency value appears to be universal [12, 19, 20].

Let us end this brief review by discussing the relationship between intermittency and the small scale “bursty” behavior of velocity increments. Indeed, it is well known in turbulence laboratory experiments that large scale increment pdf are close to be normal while small scales have larger tails. The flatness strongly increases when one goes from large to small scales. We focus only on the log-normal case, i.e., a parabolic $\zeta(q)$, extension of our considerations to other laws being straightforward. Thanks to the structure function multiscaling interpreted as a moment equality, by simply performing a time scale contraction, $\tau' = s\tau$ ($s < 1$), one can write:

$$\delta_{s\tau}X \underset{Law}{=} e^{\Omega_s} \delta_\tau X \quad (9)$$

where Ω_s is a Gaussian random variable of variance $-\lambda^2 \ln(s)$ which law is denoted as $G_s(\Omega)$. By simply assuming that for $\tau = T$ (T being the integral scale), the increments of X are normally distributed, one obtains the small scale pdf of $\delta_\tau X$ by the well known Castaing formula [21]:

$$p(z, \tau) = (2\pi)^{-\frac{1}{2}} \int G_{\tau/T}(\Omega) e^{\Omega} e^{-\frac{e^{-2\Omega} z^2}{2}} d\Omega \quad (10)$$

This means that, at scale τ , the pdf of the increments of the process $X(t)$ are obtained as a superposition of Gaussian distributions of variance $e^{2\Omega}$ where Ω is itself a gaussian random variable of variance increasing at small scales like $\lambda^2 \ln(T/\tau)$. The smaller the scale, the larger the variance of Ω and therefore the larger the tails of the increment pdf $p(z, \tau)$. The continuous deformation from Gaussian at large scales towards stretched exponential like shapes at small scales, observed in laboratory turbulence experiments, has been shown to be well accounted by the transformation (10).

B. Random cascades and logarithmic magnitude covariance

A natural question that arises after the previous analysis is how can we explicitly build models that possess multiscaling properties? In other words, since multiscaling is equivalent to intermittency, how can the variance of the magnitude increase as a logarithm of the scale as described by Eq. (8) ? The answer comes from the self-similarity Eq. (9) that can be

iterated and interpreted as a random cascade: when one goes from large to small scales, one multiplies the process by a random variable $W_s = \exp(\Omega_s)$.

Usually one starts by building a non-decreasing (i.e. with positive variations) cascade process, denoted hereafter as $M(t)$, which is often referred to as a multifractal *measure* though its variations are not bounded. More general multifractal processes (or multifractal "walks") can be simply obtained by considering a simple Brownian motion $B(t)$ (or any self-similar random process) compounded with the measure $M(t)$ considered as a stochastic time: $X(t) = B[M(t)]$. In finance literature $M(t)$ is often referred to as the 'trading time' while in turbulence $M(t)$ can be associated with the spatial or temporal distribution of energy dissipation. The statistical properties of $X(t)$ can be directly deduced from those of $M(t)$ (see e.g., [22, 23]). Random multiplicative cascades measures were originally introduced as models of the energy cascade in fully developed turbulence. After the early works of Mandelbrot [24, 25, 26], a lot of mathematical studies have been devoted to discrete random cascades [27, 28, 29, 30, 31]. Let us summarize the main properties of these constructions, set some notations and see how these notions extend to continuous cascades.

The simplest multifractal discrete cascades are the dyadic cascades defined by the following iterative rule: one starts with some interval of constant density and splits this interval in two equal parts. The density of the two sub-intervals is obtained by multiplying the original density by two (positive) independent random factors W of same law. This operation is then repeated *ad infinitum*. The integral scale corresponds to the size of the starting interval. A log-normal cascade corresponds to $W = \exp(\Omega)$ where Ω is normally distributed. Peyrière and Kahane [27] proved that this construction converges almost surely towards a stochastic non decreasing process M_∞ provided $\langle W \ln W \rangle < 1$. The multifractality of M_∞ (hereafter simply denoted as M) and of $X(t) = B(M(t))$ ($B(t)$ being a Brownian motion) has been studied by many authors (see e.g. [29]) and it is straightforward to show that the spectrum of $X(t)$ is

$$\zeta(q) = q/2 - \ln_2 \langle W^{q/2} \rangle \quad (11)$$

The self-similarity Eq. (9) for dilation factors $s = 2^n$ can also be directly deduced from the construction.

Because the discrete cascade construction involves dyadic intervals and a 'top-bottom' construction it is far from being stationary. In order to get rid of theses drawbacks, continuous cascade constructions have been recently proposed and studied on a mathematical

ground [11, 22, 23, 32, 33, 34]. They share exact multifractal scaling with discrete cascades but they display continuous scaling and possess stationary increments [11, 22, 23, 33]. Without entering into details, we just want to stress that these constructions rely upon a family of infinitely divisible random processes $\Omega_l(t)$. The process $M(t)$ is obtained as the weak limit, when $l \rightarrow 0$, of $\int_0^t e^{\Omega_l(v)} dv$. In the log-normal case, Ω_l is simply a Gaussian process defined by a covariance function that mimics the behavior of discrete cascade. Indeed, as shown in [10, 35], if $X(t) = B(M(t))$ where $M(t)$ is a discrete cascade as defined previously with intermittency coefficient λ^2 , then correlation function $\rho(\Delta t)$ of the magnitude $\omega_\tau(u) = \ln(|\delta_\tau X(u)|)$ decreases slowly as a logarithm function:

$$\rho(\Delta t) \stackrel{def}{=} Cov[\omega_\tau(u), \omega_\tau(u + \Delta t)] \simeq -\lambda^2 \ln\left(\frac{\Delta t}{T + \tau}\right) \text{ for lags } \Delta t \leq T. \quad (12)$$

The integral scale T where cascading process “starts” can therefore be interpreted as a *correlation length* for the variation log-amplitudes of $X(t)$. The so-called Multifractal Random Walk (MRW) process introduced in Ref. [36] consists in constructing a log-normal multifractal process $X(t) = B(M(t))$ where $B(t)$ is a Brownian motion and

$$M(t) = \lim_{l \rightarrow 0^+} \int_0^t e^{\Omega_l(u)} du \quad (13)$$

where the $\Omega_l(u)$ is a gaussian process with a logarithmic covariance as given in Eq. (12). In Fig. 1(a) and 1(b) are plotted respectively a sample of a log-normal measure $M(dt)$ ($dt = 1$) and a path of a MRW process $X(t)$ corresponding to $\lambda^2 = 0.025$ and $T = 512$.

The studies devoted to continuous versions of discrete cascades have mainly shown that multifractal processes are related to exponential of logarithmic correlated random processes. The magnitude covariance function has been proven to be at the heart of the notion of “continuous cascade”. As we shall see below, it also allows one to estimate the intermittency coefficient in a more reliable way than methods based on scaling properties.

C. Intermittency coefficient estimation issues

As far as the problem of the estimation of the intermittency coefficient is concerned, it results from previous discussion that this coefficient, originally defined as the curvature of $\zeta(q)$ (Eq. (3)), can be estimated either from the behavior of magnitude variance across scales (Eq. (8)) or from the slope of the time magnitude covariance in lin-log coordinates (Eq. (12)).

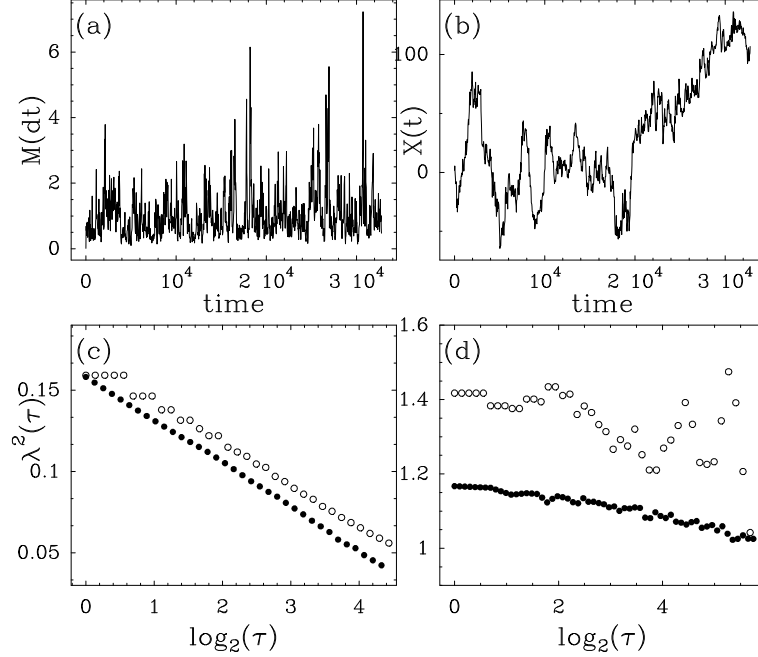


FIG. 1: Estimation of the intermittency coefficient for a log-normal MRW multifractal measure (a) and a log-normal MRW process (b). In both cases the sample size is 32768 points, $\lambda^2 = 0.025$ and $T = 512$. In (c) are plotted the magnitude covariance (●) and magnitude variance (○) as a function respectively of the logarithm of the lag and the logarithm of the scale. The slope of both curves provides an estimation of λ^2 . One can see that for measure $M(dt)$, the errors in the estimation are comparable. In (d) are displayed the same plots as in (c) but for the magnitude of the MRW process. Because of the additive noise and the small number of independent points at large scales, the estimation relying upon the magnitude variance turns out to be much more altered.

Let us show that this latter definition is much more reliable than former one. The precise computation of the properties of estimators relying upon Eqs (8) and (12) is a difficult task. In Ref. [37], it has been shown that a Generalized Method of Moments relying on the magnitude correlation function provides an unbiased and consistent estimator of λ^2 . Estimators relying on Eq. (8) have been precisely discussed within the context of atmospheric turbulence in Ref. [19] where the authors showed that it allowed one, by means of a bootstrap method called “surrogate analysis”, to estimate λ^2 and distinguish intermittent from non intermittent time series.

A simple argument allows us to understand why magnitude covariance based estimation

(Eq. (12)) is better than scale magnitude cumulant analysis (Eq. (8)) in the case of multifractal random walks. This is illustrated in Fig. 1 where both estimators are compared for a sample of a multifractal random measure constructed from a log-normal continuous cascade (Fig. 1(a)) and a MRW process (Fig. 1(b)). One sees in Fig. 1(c), that in the case one handles directly the random cascade measure, both estimators are roughly equivalent. However, in the case of a MRW process, the measure is not directly observed since it represents the stochastic variance of the random walk. In this situation, the estimates based on magnitude covariance are better than those obtained from the magnitude variance scaling (Fig. 1(d)). This feature can be explained as follows: if one considers that for continuous cascades processes, Eq. (9) is an equality in law for all finite dimensional distributions (f.d.d.), by taking the logarithm, one gets:

$$\omega_\tau(u) = \ln(|\delta_\tau X(u)|) \underset{\text{f.d.d.}}{=} \Omega_\tau(u) + \ln(|\epsilon(u)|) \quad (14)$$

where $\Omega_\tau(u)$ is a log-correlated gaussian random variable (Eq. (12)) which variance behaves like in Eq. (8) while $\epsilon(u)$ is a standardized normal white noise independent of Ω_τ . Note that in the case of a multifractal measure, there is no noise term $\ln(|\epsilon|)$ and the estimation error is small as compared to the situation of MRW when this term is present. One can then assume that the estimation error mainly comes from the presence of $\ln(|\epsilon|)$. This error is thus expected to decrease, in both cases, as $\frac{1}{\sqrt{N_e}}$ if N_e is the number of effective independent samples of the considered signal. This effective number is proportional to the overall sample size but decreases with the scale τ . Therefore, since at scale τ , the effective number of independent points is $N_e \simeq N\tau^{-1}$, if one fits Eq. (8) over the range of scale extending from $\tau = 1$ to $\tau = \tau_{\max}$, the mean error is roughly proportional to $\sqrt{\tau_{\max} N^{-1}}$. On the other hand, by fitting Eq. (12) at scale $\tau = 1$ from lags $\Delta t = 1$ to $\Delta t = \tau_{\max}$, one expects an approximately constant error of $\sqrt{N^{-1}}$. Moreover, the error in the computation of the variance is proportional to the square root fourth moment of $\ln(\epsilon)$ while the error in the covariance is proportional to the second moment. Since the ratio between these two quantities is 3, the ratio of errors between the two methods is of order:

$$r \simeq 3\sqrt{\tau_{\max}} \quad (15)$$

Let us notice that, rigorously, the error also depends on the overall range of values used to apply the linear regression and thus one expects, in the case of an estimation relying

upon Eq. (8), there is an optimal range of scale to perform the fit. This optimum results, on the one hand, from a reduction of the error when one increases the fitting range of scales and, on the other hand, from the increasing of the error associated with the small number of independent points at large scales (see Ref. [38] where such a problem is considered in details). We have performed extensive Monte-Carlo estimations using synthetic log-normal continuous cascades and we have checked that for parameters, sample sizes and range of scales close to the experimental values considered below (see section III), the observed ratio between the errors is $r_{exp} \simeq 10$ in agreement with previous considerations. The intermittency coefficient of a random cascade is thus estimated in a much more reliable way using magnitude correlation functions.

D. Squared log magnitude covariance as the result of Lagrangian and Eulerian intermittency

In most fluid mechanics experiments, one usually records one or several components of the velocity field using an anemometer, so one has only access to the values of the field at a fixed spatial position as a function of time. In order to make inferences on the spatial properties of the velocity, i.e., the Eulerian field, one generally invokes the Taylor Frozen hypothesis or, when the turbulence rate is large, the Tenekes sweeping argument according to which small scale velocity fluctuations are mainly caused by Eulerian variations advected by large scale random motions [39]. However, as explained below, for some functions, single point measurements cannot be linked so easily to their Eulerian counterpart. Hereafter, we reproduce the argument of B. Castaing [40, 41] in order to understand the shape of the single point magnitude covariance if one supposes that both Eulerian and Lagrangian velocity fluctuations are given by a continuous cascade as described previously.

Let us denote $\Omega(x, t)$ the magnitude at time t and position x . It is important to notice that $\Omega(x, t)$ is a local field that does not depend on any spatial or time scale (for example in turbulence, $\Omega(x, t)$ can be considered as the logarithm of the dissipation field or of the velocity increments at a scale smaller than the Kolmogorov dissipation scale).

Our goal is to compute

$$\text{Cov} [\Omega(x, t), \Omega(x, t + \Delta t)] \tag{16}$$

as a function of the time lag Δt for a fixed value of x .

If one supposes that both Eulerian and Lagrangian fields Ω are log-correlated, i.e., well described by a continuous cascade model, then

$$\begin{aligned}\text{Cov} [\Omega(x, t), \Omega(x + r, t)] &= \lambda^2 \ln\left(\frac{L}{r + \eta_e}\right) \\ \text{Cov} [\Omega(x(t), t), \Omega(x(t + \Delta t), t + \Delta t)] &= \mu^2 \ln\left(\frac{T}{\Delta t + \eta_l}\right)\end{aligned}$$

where Δt and r are time and space lags, η_e and η_l are small scale spatial and temporal cut-offs (i.e. the Kolmogorov scales in turbulence), L and T are spatial and temporal integral scales and λ^2 , μ^2 are Eulerian and Lagrangian intermittency coefficients.

Let us suppose that the fluid particle at position x at time $t + \Delta t$ was at position x' at time t . Thanks to the above covariance formula, one can write:

$$\Omega(x, t + \Delta t) = \rho_1 \Omega(x', t) + \epsilon \quad (17)$$

where ϵ is a random variable independent of $\Omega(x', t)$ and:

$$\rho_1 = \frac{\mu^2 \ln\left(\frac{T}{\Delta t + \eta_l}\right)}{\text{Var}(\Omega)} \quad (18)$$

But (at least from a statistical point of view) $r = |x' - x| = V\Delta t$ where V is a 'typical' velocity (the mean or r.m.s. velocity) so that, if one assumes that $L \simeq VT$:

$$\Omega(x', t) = \rho_2 \Omega(x, t) + \epsilon' \quad (19)$$

where ϵ' is a random variable independent of $\Omega(x, t)$ and:

$$\rho_2 = \frac{\lambda^2 \ln\left(\frac{VT}{V\Delta t + \eta_e}\right)}{\text{Var}(\Omega)} \quad (20)$$

Then, if ϵ and ϵ' are uncorrelated, since the correlation coefficient between $\Omega(x, t)$ and $\Omega(x, t + \Delta t)$ is the product $\rho_1 \rho_2$, we have

$$\text{Cov} [\Omega(x, t), \Omega(x, t + \Delta t)] = \text{Var}(\Omega) \rho_1 \rho_2, \quad (21)$$

and by taking into account the fact that $\text{Var}(\Omega_s) = \mu^2 \ln(T/\eta_l) = \lambda^2 \ln(L/\eta_e)$ one obtains finally, for lags such that $V\Delta t \gg \eta_e$ and $\Delta t \gg \eta_l$:

$$\text{Cov} [\Omega(x, t), \Omega(x, t + \Delta t)] \simeq \frac{\lambda^2}{\ln\left(\frac{T}{\eta_l}\right)} \ln^2\left(\frac{\Delta t}{T}\right) = \frac{\mu^2}{\ln\left(\frac{L}{\eta_e}\right)} \ln^2\left(\frac{\Delta t}{T}\right). \quad (22)$$

If one plots $\sqrt{\text{Cov}}$ as a function of $\ln(\tau)$ one expects a straight line of slope:

$$r = \sqrt{\frac{\lambda^2}{\ln \frac{T}{\eta_l}}} = \sqrt{\frac{\mu^2}{\ln \frac{L}{\eta_e}}} \quad (23)$$

In one knows the “Reynolds numbers” $\frac{L}{\eta_e}$ and $\frac{T}{\eta_l}$, the intermittency coefficients can be estimated from the slope r as:

$$\lambda^2 = r^2 \ln\left(\frac{T}{\eta_l}\right) \quad (24)$$

$$\mu^2 = r^2 \ln\left(\frac{L}{\eta_e}\right) \quad (25)$$

We see that, by taking into account both Eulerian and Lagrangian fluctuations on single point measurements, one should observe a squared logarithm magnitude covariance instead of the logarithmic behavior of Eq. (12). This peculiar shape of magnitude covariance has indeed been precisely observed on laboratory fully developed turbulence data in Ref. [12].

III. RESULTS: INTERMITTENCY IN MESOSCALE WIND FLUCTUATIONS

A. The data series

The results reported in the following are based on different wind velocity time series. The first data set consists in horizontal wind speeds and directions that have been recorded every minutes during 5 years (1998-2002) at our laboratory in Ajaccio - Vignola at a height of 10 m by means of a cup anemometer. We also study hourly wind speed and direction data (10 minutes averages) for 7 different sites in Corsica (France). The length of these series is also 5 years. These data have been measured and collected by the French Meteorological Service of Climatology (Meteo-France) using a cup anemometer and wind vane at 10 meters above ground level. Finally, we also consider potential winds from KNMI HYDRA PROJECT available online [42]: they represent series of hourly (1 hour average), 10 meters potential wind speed gathered during several years at various locations in Netherlands. More specifically we consider the series recorded at 3 different sites over a long period of several decades. Table I summarizes the main characteristics of the studied series.

In the sequel, $v(t)$ will denote the modulus of the velocity horizontal vector while $v_x(t)$ and $v_y(t)$ will stand for its two components along arbitrary orthogonal axes x and y . We

Location	Latitude	Longitude	Dates	Sampling freq.	Site
Vignola (Ajaccio)	41°56'N	8°54'E	1998-2003	1 min	50m, coastal, high hills
Ajaccio	41°55'N	8°47'E	2002-2006	1 hour	5m, coastal, plain, airport
Bastia	42°33'N	9°29'E	2002-2006	1 hour	10m, coastal, plain, airport
Calvi	42°31'N	8°47'E	2002-2006	1 hour	57m, coastal, hills
Conca	41°44'N	9°20'E	2002-2006	1 hour	225m, high hills
Figari	41°30'N	9°06'E	2002-2006	1 hour	21m, plain, airport, hills
Renno	42°11'N	8°48'E	2002-2006	1 hour	755m, mountains
Sampolo	41°56'N	9°07'E	2002-2006	1 hour	850m, mountains
Eindhoven	51°44'N	5°41'E	1960-1999	1 hour	20m, plain
Ijmuiden	52°46'N	4°55'E	1956-2001	1 hour	4m, coastal, plain
Schipol	52°33'N	4°74'E	1951-2001	1 hour	-4m, plain, airport

TABLE I: Main features of the time series

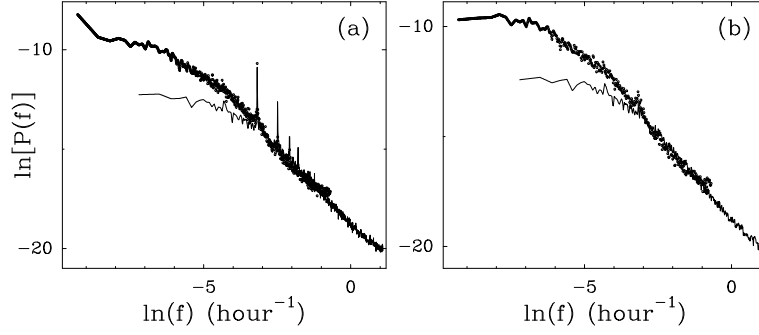


FIG. 2: Power spectrum density of v_x wind components 10 min rate Vignola series (solid line) and hourly Eindhoven series (dotted line) in log-log representation. (a) One clearly identifies the peaks associated with diurnal oscillation superimposed to an overall scaling regime where $P(f) \sim f^{-\beta}$ with $\beta \simeq 1.6$. This regime roughly extends from few days to few minutes. Turbulent atmospheric scales are below the finest resolved time scale. (b) Plot of the same spectra where the estimated local seasonal components have been removed.

have by definition:

$$v(t) = \sqrt{v_x(t)^2 + v_y(t)^2}$$

Because there is no well defined constant mean velocity direction with a small turbulent rate, we have chosen to study v_x and v_y separately instead of considering meaningless longitudinal and transverse components.

The power spectrum analysis is one of the most common tools for analyzing random functions and is at the heart of a wide number of studies of wind velocity statistics. Since

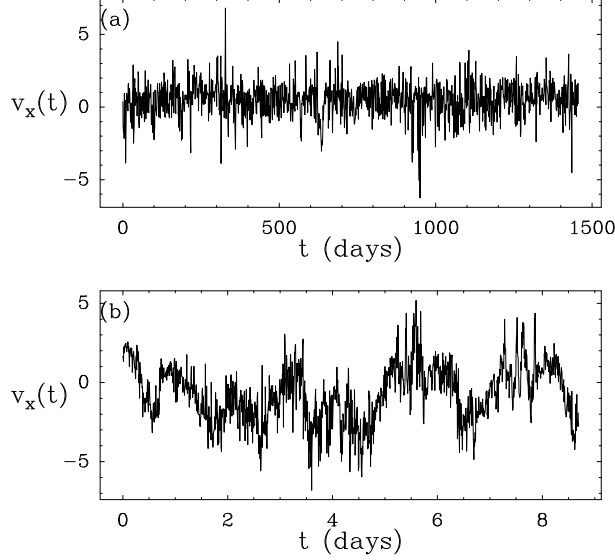


FIG. 3: Time fluctuations of the $v_x(t)$ component of the Vignola velocity field. (a) At large time scales, one does not see any structure, we are in the flat (white noise) regime of the power spectrum. (b) At a finer time resolution, the series appears as a superposition of turbulent gusts and a more regular component.

the pioneering work of Ven Der Hoven [43, 44], the shape of a typical atmospheric wind speed spectrum in the atmospheric boundary layer is still matter of debate. It is relatively well admitted that it possesses two regimes separated by low energy valley called the “spectral gap” located at frequencies around few minutes. This gap separates the microscale regime, where turbulent motions take place, from the mesoscale range. In the homogeneous turbulent regime, it is well known that the spectrum associated with the velocity field behaves like $E(k) \sim k^{-5/3}$ as predicted by Kolmogorov in 1941 [1] (k is the spatial wave-number). In the mesoscale range, for time scales greater than few minutes, the shape of this spectrum appears to depend on various factors. If some experiments suggest that a $k^{-5/3}$ spectrum can extend up to synoptic scales [45, 46] in the free atmosphere, things are different in the surface layer [47]. Some authors suggest that statistics a priori depend on local conditions (orographic, atmospheric,...) and one does not expect the same degree of universality as in the microscale regime. For example, in ref [3], it is shown that the spectrum exponent may depend on the atmospheric stability conditions and also on the topography.

In Fig. 2 are plotted the power spectrum of the v_x component of two series: the “high

frequency” (10 min rate) series of Vignola and the hourly series recorded at Eindhoven. These two spectra that do not cover the same frequency range have been shifted by an arbitrary multiplicative factor. Series associated with the v_y component or corresponding to other sites have similar features. One can see that, up to the mains peaks associated with diurnal wind oscillations (see below), these spectra are well described by a power-law $P(f) \sim f^{-\beta}$ in a frequency domain which corresponds to time scales from few minutes to a characteristic time of few days (note that the low frequency behavior is much more reliable in the Eindhoven series since it covers a period close to ten time longer than the Vignola series). The value of the exponent is $\beta \simeq 1.6$ for both sites. Within the framework of self-similar Gaussian processes [48], the fact that $\beta > 1$ for all series indicates that the signal process $v_x(t)$ has continuous paths. Since at low frequency the spectrum becomes flat, this means that the process appears regular at small scales and more “noisy” at larger scales. This feature is illustrated in Fig. 3 where we have plotted two samples of the component $v_x(t)$ of Vignola wind series over two different time intervals. At very large scale, the signal looks like a highly irregular “white noise” that corresponds to the power-spectrum low frequency flat behavior (Fig. 3(a)) while a zoom over a finer time interval reveals more regular variations (Fig. 3(b)). Notice that one can also observe a daily oscillating behavior and high frequency turbulent gusts superimposed to these regular random variations.

Since our goal is to study the stationary random components of the velocity field, we have preprocessed all time series in order to remove the seasonal components. In fact the diurnal oscillations $S_{x,y}$ are not really periodic but vary during the year according to the sun position. We have used a local harmonic parametrization of these components and computed the parameters by minimizing an exponential moving average of a quadratic error (see [49, 50] for more details). In order to study the fluctuations in these deseasonalized series and an eventual intermittency, we can compute, as in turbulence literature, its increments. Notice that one can alternatively study velocity component wavelet coefficients or, if one wants to account for the low-frequency behavior, the error in the one step forward prediction of a Langevin like modeling of $v_x(t)$ and $v_y(t)$ [50]:

$$v_{x,y}(t+1) = S_{x,y}(t+1) + (1-\gamma)(v_{x,y}(t) - S_{x,y}(t)) + w_{x,y}(t) \quad (26)$$

where the friction coefficient γ is estimated to be $\gamma \simeq 1 \text{ day}^{-1}$, $S_{x,y}(t)$ stands for the seasonal additive component of the wind velocity and $w_{x,y}(t)$ is the error (noise) term. Whatever the

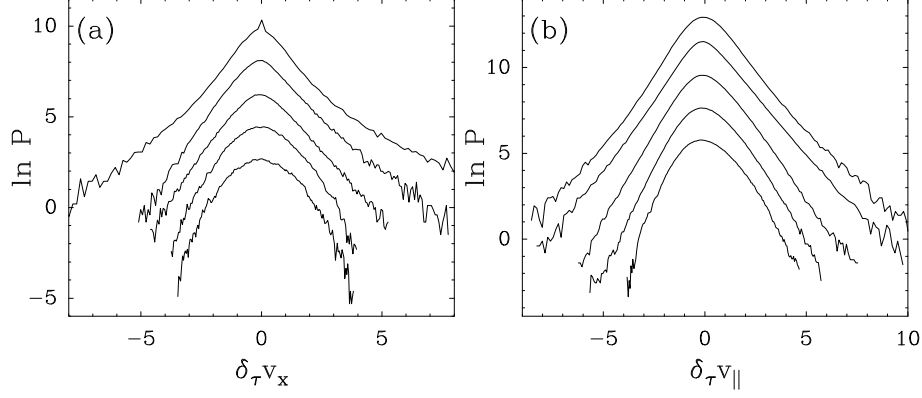


FIG. 4: Semi-logarithmic representation of standardized velocity increment pdf at various scales. From top to bottom one goes from small to coarse time scales. All graphs have been vertically shifted for sake of clarity. (a) Logarithm of the pdf of the wind velocity increments $\delta_\tau v_x$ for the Eindhoven wind series. Time scales τ go from 1 hour to 5 days. (b) Same plots as in (a) but for the increments of the longitudinal velocity field $\delta_\tau v_{||}$ in a high Reynolds number turbulence experiment (see text). Scales τ extend from the Kolmogorov scale to the integral scale.

precise definition used to compute the local fluctuations, the results presented in the next section remain unchanged.

B. Evidences for a mesoscale cascade

As recalled in the introduction, unlike inertial subrange turbulence, few papers have been devoted to the study of scaling properties of atmospheric fields from moderate to large scales. In Ref. [4], the authors find that cloud satellite data display multiscaling over the range $1 - 5 \cdot 10^3$ km and suggest the existence of a (anisotropic) cascade process from planetary scales down to the microscales. As far as scaling properties of surface layer wind speed are concerned, some studies focus on (multi-) scaling properties. In Ref. [7], the authors use Detrended Fluctuation Analysis on various hourly averaged wind series and provide evidences of a cross-over between two scaling regimes separating mesoscale range from very large scale range. The scale of the cross-over was found to be $T \simeq 5$ days and the author conjectured the possibility of the existence of multiscaling for scales below this scale. In that case the scale T could be identified to some integral (injection) scale. In the Refs. [3, 51],

Lauren *et al.* perform an analysis and a modeling of atmospheric wind in both mesoscale and microscale (turbulent) regimes. They show that the concepts of multiscaling and cascades are also pertinent for characterizing and simulating low-wavenumbers properties of surface layer winds.

Though the above mentioned studies provide hints for the existence of intermittency in wind fluctuations at large scales, as explained in section II, because of diurnal oscillations, discreteness of the data, limited size of the scaling range and for purely statistical considerations, the reported estimations of (multi-) scaling properties of mesoscale wind data are far from being reliable. A more direct and convincing illustration of the intermittent nature of mesoscale wind variations is provided in Fig. 4(a) where we have plotted the normalized pdf of the increments of (deseasonalized) wind components v_x of the Eindhoven site in logarithmic scale. One sees that increment distributions go from ‘stretched exponential’ like functions (with large tails) to Gaussian like behavior (parabola) when going from 1 hour to few days time scales. This behavior is very similar to the features observed in fully developed turbulence laboratory experiments. In Fig. 4(b), for comparison purpose, we have plotted in the same logarithmic scale, the standardized pdf of longitudinal velocity increments computed from experimental data obtained by B. Chabaud and B. Castaing in a low temperature gaseous Helium jet experiment [52] (the Taylor scale based Reynolds number is $R_\lambda = 929$). As the scale τ varies from the dissipation to the integral scale, one observes the same deformation of the pdf from large tailed shape to Gaussian-like shape. As explained in section II A (Eq. (10)), such a variation of the pdf behavior across scales is usually associated with the existence of an intermittent cascade. Let us notice that the smallest time scales we considered, correspond to scales greater than or equal to the “injection” largest scale of atmospheric boundary layer turbulence. Consequently, according to our observations, velocity increment statistics at large (atmospheric surface layer) turbulent scales are characterized by a strong kurtosis. This contrasts with the situation in laboratory experiments where the distribution are nearly gaussian at large scales (as illustrated by the bottom graph in Fig. 4(b)). Similar observations have been performed in [8, 9]. In [8], the authors interpret the intermittency of large scale atmospheric turbulence by the fluctuations of the turbulence intensity at this scale. The velocity mean is no longer constant but stochastic. Similar observations on the vorticity field have been made in [9]. In the following, we suggest that these fluctuations of turbulence intensity can be interpreted as

the result of a cascading process starting at a larger time scale.

As advocated in section II C, the best way to reveal the presence of an underlying random cascade and to estimate the intermittency coefficient is to study the magnitude correlations functions associated with velocity small scale variations. If one writes equation (14) for the small scale increments of respectively v_x and v_y (where the seasonal components have been removed) one can define two magnitude processes and two processes Ω_x and Ω_y :

$$\begin{aligned}\omega_{x,\tau}(t) &\equiv \ln(|\delta_\tau v_x(t)|) = \Omega_{x,\tau}(t) + \ln(|\epsilon_x(t)|) \\ \omega_{y,\tau}(t) &\equiv \ln(|\delta_\tau v_y(t)|) = \Omega_{y,\tau}(t) + \ln(|\epsilon_y(t)|)\end{aligned}$$

If one assumes that the noises ϵ_x and ϵ_y are independent gaussian white noises, then thanks to the fact that $\text{Var}(\ln(|\epsilon|)) \simeq 1.23$, one can compute the correlation coefficient of Ω_x and Ω_y from the correlation of ω_x and ω_y . The obtained results for all data series are summarized in table II. One clearly sees that the correlation coefficient of magnitude processes is for all series close to 20 % while the estimated coefficients for the Ω components are close to 1². This result strongly suggests that the processes Ω_x and Ω_y are identical and therefore Ω is a scalar quantity. One thus has (up to season components):

$$\begin{aligned}\delta_\tau v_x(t) &= e^{\Omega_\tau(t)} \epsilon_x(t) \\ \delta_\tau v_y(t) &= e^{\Omega_\tau(t)} \epsilon_y(t) .\end{aligned}$$

The scalar $e^{\Omega_\tau(t)}$ is simply the (stochastic) amplitude of velocity fluctuation vector at scale τ .

According to these findings, in the following we compute a surrogate of the scalar process $\Omega(t)$ as follows:

$$\Omega_\tau(t) = \frac{1}{2} \ln (\delta_\tau v_x(t)^2 + \delta_\tau v_y(t)^2) \quad (27)$$

which is less noisy than individual magnitudes ω_x or ω_y . Let us notice, as already mentioned, that if one replaces in previous analysis, $\delta_\tau v_{x,y}$ by the error term in a Langevin model of $v_{x,y}$ as in Eq. (26) or by small scale wavelet coefficients, all the results remain unchanged [50]. Since the results presented below do not depend on the chosen small scale τ (we focus

² notice that estimated coefficients greater than 1 are probably due to our hypothesis concerning the normality of $\epsilon_{x,y}$; such an assumption can only be a rough approximation for some series because of finite size and granularity effects

Location	ω correlations	Ω correlations
Vignola (Ajaccio)	0.19	1.16
Ajaccio	0.22	1.31
Bastia	0.20	1.10
Calvi	0.14	1.10
Conca	0.22	1.07
Figari	0.17	1.32
Renno	0.21	0.71
Sampolo	0.11	0.68
Eindhoven	0.22	1.01
Ijmuiden	0.22	0.99
Schipol	0.21	0.98

TABLE II: Correlation coefficients of magnitude components for the different sites

on properties involving mainly lags greater than τ), we omit any reference to this scale and denote $\Omega(t)$ the local "magnitude" estimated at small scale according to Eq. (27).

The process $\Omega(t)$ also possesses a seasonal component which means that seasonal effects manifest not only through an additive (locally) periodic component but also through a diurnal modulation of the velocity stochastic amplitude. This multiplicative seasonal component has been estimated using the same local least squared method as for the additive components [50]. In the following, we assume that all seasonal effects have been removed from the estimated field $\Omega(t)$.

Along the line of the method described in section II C, we have estimated the magnitude $\Omega(t)$ correlation functions $\rho(\Delta t) = \text{Cov}(\Omega(t), \Omega(t + \Delta t))$ for all the time series. As illustrated in Fig. 5, when one plots $\rho^{1/2}(\Delta t)$ as a function of $\ln(\Delta t)$ one observes, for all series, a decreasing linear function that becomes zero above some lag T . It is striking to observe that all slopes are close to each other and that the "correlation" scale (integral scale) is roughly the same for all sites. In order to handle less noisy curves, we have plotted in Fig. 6(b), within the same representation, the mean correlation function for all sites in Corsica, for all sites in Netherlands and for the high frequency series at Vignola (in Fig. 6(a) the same graphs are displayed using a linear representation). Up to some remaining bump around the lag of one day due to the non perfect removing of the seasonal components, one observes a well defined linear dependence on a range $[\ln(\tau), \ln(T)]$. This means that for all wind

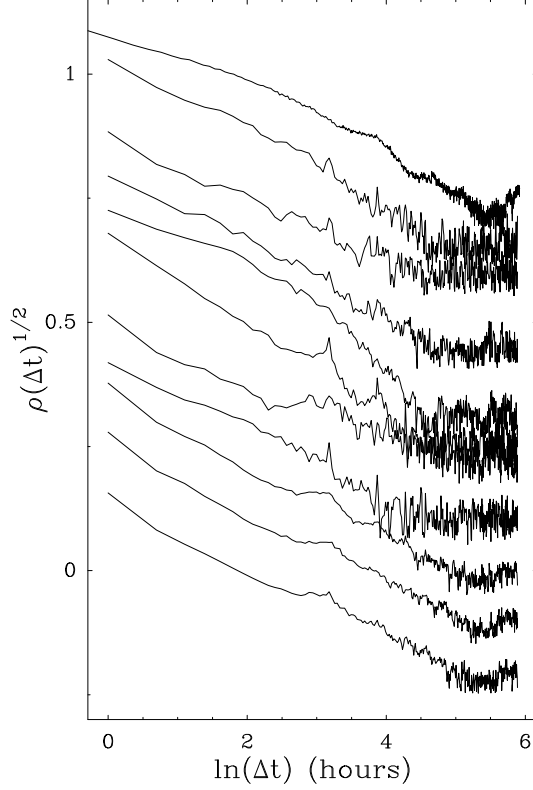


FIG. 5: Square root of magnitude covariance functions estimated for all wind series. The three bottom graphs correspond to Netherlands hourly series while the top graph is correlation of magnitudes associated with the 'high frequency' Vignola data series. All the graphs have been arbitrary shifted vertically for clarity purpose. One can observe comparable values of the parameters β^2 and T (see text).

series, the covariance of $\Omega(t)$ reads ($\Delta t > \tau$):

$$\rho(\Delta t) = \beta^2 \ln^2\left(\frac{T}{\Delta t}\right)$$

In section IID, we have explained how such a square logarithmic dependence of the single point covariance can be the result of log-correlated Eulerian and Lagrangian fields. This feature has also been observed on various laboratory turbulence data [12, 40]. These observations are therefore direct evidences that a random cascade mechanism can be involved in the energy transfer at scales much greater than the usual turbulent microscale. Let us remark that the value of the integral scale we found is $T \simeq 5$ days in Holland and Corsica and the value of the slope $\beta \simeq 0.07$. In order to deduce Eulerian (or Lagrangian) value of the intermittency coefficients, one would need to know the value of $\frac{T}{\eta}$ where η is a small

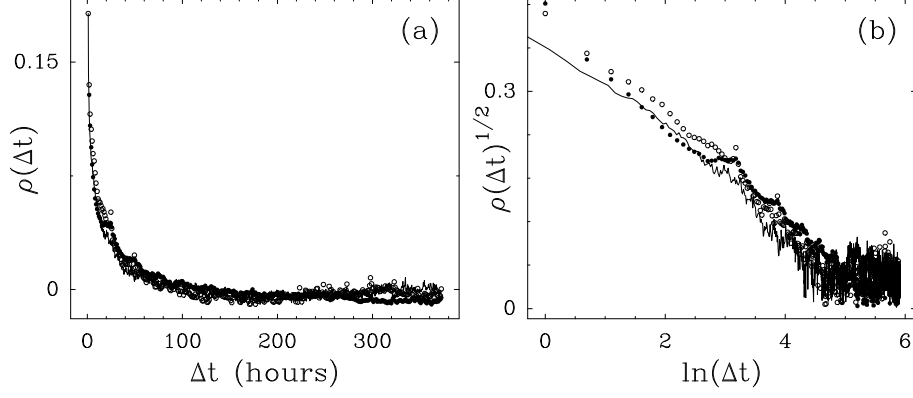


FIG. 6: Mean magnitude correlation functions associated with wind series in Corsica (\circ) and Netherland (\bullet). The solid line represents the magnitude covariance of the Vignola series (10 min rate). (a) The graphs are in linear scales. (b) The square root of the covariances are represented as function of the logarithm of the time lag Δt .

time scale cut-off above which Lagrangian variations are no longer intermittent. For example if one sets $T \simeq 5$ days and one chooses η to be a typical time scale separating micro and meso scales, i.e., $\eta \simeq 10$ min, according to Eq. (24) one gets an Eulerian intermittency coefficient $\lambda^2 \simeq 0.03$, i.e., very close to the value found for fully developed turbulence (see e.g., [12, 19, 20]).

IV. CONCLUSION AND PROSPECTS

The goal of this paper was to provide evidences that the surface layer wind fluctuation statistics in the mesoscale range are, very much like microscale turbulent statistics, characterized by strongly intermittent properties. We have first reviewed how the intermittency of continuous random cascades can be advantageously studied using magnitude correlation analysis as compared to standard scaling or magnitude cumulant estimations. Within this framework and using various wind velocity and direction time series in Corsica (France) and Netherlands, we have shown that one can define a scalar magnitude field that displays "universal" squared log correlation functions. Such peculiar shape of time correlation functions at a fixed position is shown to result from a continuous cascade (with log-correlated magnitude) that governs the fluctuations in both Eulerian and Lagrangian frames. The same behavior has been observed in laboratory turbulence experiments. The existence of some

mesoscale "energy cascade" and other similarities with the 3D isotropic turbulence properties, raises various fundamental questions. Unlike synoptic circulations, mesoscale motions can be associated with a wide variety of phenomena covering a large range of characteristic scales from thunderstorms, mountain waves to front dynamics. In that respect, the "universal" features discussed in this paper have to be confirmed using further experimental data. Let us note however that a characteristic time scale of few days is usually associated with front dynamics [2] and some comparable typical time scales have been already reported in the literature [5, 7]. From a practical point of view our findings lead to a better characterization of the statistical properties of wind fluctuations. The framework of intermittent statistics and random cascade models can be applied to address problems related to wind resources assessing, extreme events characterization or to design a simple stochastic model in order to perform short term wind predictions [50, 53].

Acknowledgments

We acknowledge "Royal Netherlands Meteorological Institute" [42] for the availability of the potential wind speed data in Netherlands and B. Chabaud and B. Castaing for the permission to use their experimental turbulence data.

-
- [1] U. Frisch, *Turbulence* (Cambridge Univ. Press, Cambridge, 1995).
 - [2] J. Holton, *An introduction to Dynamic Meteorology* (Elsevier Academic Press, Burlington, 2004).
 - [3] M. K. Lauren, M. Menabde, A. W. Seed, and G. Austin, *Boundary-Layer Meteorol.* **90**, 21 (1999).
 - [4] S. Lovejoy, D. Schwertzer, and D. Stanley, *Phys. Rev. Lett.* **86**, 5200 (2001).
 - [5] V. Gupta and E. Waymire, *J. Geophys. Res.* **95**, 1999 (1990).
 - [6] V. Gupta and E. Waymire, *J. Appl. Meteor.* **32**, 251 (1993).
 - [7] R. G. Kavasseri and R. Nagarajan, *IEEE Trans. on Circuits and Systems. Fundam. Theory and Apps* **51**, 2262 (2004).
 - [8] F. Bottcher, S. Barth, and J. Peinke, *St. Env. Res. and Risk Assessment* **21**, 299 (2006).

- [9] M. Kholomyansky, L. Moriconi, and A. Tsinober, Phys. Rev. E **76**, 026307 (2007).
- [10] A. Arneodo, J. F. Muzy, and D. Sornette, European Physical Journal B **2**, 277 (1998).
- [11] J.-F. Muzy, J. Delour, and E. Bacry, Eur. J. Phys. B **17**, 537 (2000).
- [12] J. Delour, J. Muzy, and A. Arneodo, Eur. Phys. J. B **23**, 243 (2001).
- [13] E. Bacry, A. Kozhemyak, and J. F. Muzy, Journal of Economic Dynamics and Control **32**, 156 (2008).
- [14] A. Kozhemyak, *Modélisation de séries financières à l'aide de processus invariants d'échelle. Application à la prédiction du risque*, Ph.D. thesis, Ecole Polytechnique, Palaiseau, France (2006).
- [15] J. Delour, *Processus aléatoires auto-similaires: applications en turbulence et en finance*, Ph.D. thesis, Université de Bordeaux I, Pessac, France (2001).
- [16] F. Anselmet, R. Antonia, and L. Danaila, Planetary and Space Science **49**, 1177 (2001).
- [17] B. Lahermes, P. Abry, and P. Chainais, Int. J. of Wavelets, Multiresolution and Inf. Processing **2**(4), 497 (2004).
- [18] J. Muzy, E. Bacry, R. Baile, and P. Poggi, Europhys. Lett. **82**, 60007 (2008).
- [19] S. Basu, E. Foufoula-Georgiou, B. Lashermes, and A. Arneodo, Phys. Fluids **19**, 115102 (2007).
- [20] A. Arneodo, S. Manneville, and J. Muzy, Eur. Phys. J. B **1**, 129 (1998).
- [21] B. Castaing, Y. Gagne, and E. Hopfinger, Physica D **46**, 177 (1990).
- [22] J.-F. Muzy and E. Bacry, Phys. Rev. E **66**, 056121 (2002).
- [23] E. Bacry and J.-F. Muzy, Comm. in Math. Phys. **236**, 449 (2003).
- [24] B. B. Mandelbrot, Journal of Fluid Mechanics **62**, 331 (1974).
- [25] B. B. Mandelbrot, C.R. Acad. Sci. Paris **278**, 289 (1974).
- [26] B. B. Mandelbrot, Journal of Statistical Physics **110**, 739 (2003).
- [27] J. P. Kahane and J. Peyrière, Adv. in Mathematics **22**, 131 (1976).
- [28] Y. Guivarc'h, C.R. Acad. Sci. Paris **305**, 139 (1987).
- [29] G. M. Molchan, Comm. in Math. Phys. **179**, 681 (1996).
- [30] G. M. Molchan, Phys. Fluids **9**, 2387 (1997).
- [31] Q. Liu, Asian Journal of Mathematics **6**, 145 (2002).
- [32] F. Schmitt and D. Marsan, European Physical Journal B **20**, 3 (2001).
- [33] J. Barral and B. B. Mandelbrot, Prob. Theory and Relat. Fields **124**, 409 (2002).

- [34] P. Chainais, R. Riedi, and P. Abry, IEEE transactions on Information Theory **51**, 1063 (2005).
- [35] A. Arneodo, E. Bacry, S. Manneville, and J. Muzy, Phys. Rev. Lett. **80**, 708 (1998).
- [36] J. F. Muzy, J. Delour, and E. Bacry, Eur. J. Phys. B **17**, 537 (2000).
- [37] E. Bacry, A. Kozhemyak, and J. F. Muzy, *Log-normal continuous cascades: aggregation properties and estimation* (2009), quantitative Finance (in press).
- [38] B. Audit, E. Bacry, J. Muzy, and A. Arneodo, IEEE Trans. Info. Theory **48**, 2938 (2002).
- [39] L. Chevillard, S. Roux, E. Leveque, N. Mordant, J. Pinton, and A. Arneodo, Phys. Rev. Lett. **95**, 064501.1 (2005).
- [40] B. Castaing, Eur. Phys. J. B **29**, 357 (2002).
- [41] B. Castaing, Phys. Rev. E **73**, 068301 (2006).
- [42] See www.knmi.nl/samenw/hydra/index.html.
- [43] I. V. der Hoven, J. of Meteorol. **14**, 160 (1957).
- [44] A. H. Oort and A. Taylor, Month. Weather Rev **97**, 623 (1969).
- [45] G. Nastrom, K. Gage, and W. Jasperson, Nature **310** (1983).
- [46] D. Lilly, J. Atmos. Sci. **40** (1983).
- [47] J. Kaimal, J. Atmos. Sci. **35**, 18 (1978).
- [48] M. Taqqu and G. Samorodnisky, *Stable Non-Gaussian Random Processes* (Chapman & Hall, New-York, 1994).
- [49] B. Abraham and J. Ledolter, *Statistical methods for forecasting* (J. Wiley & Sons, New-York, 1983).
- [50] R. Baile, J. Muzy, and P. Poggi, *Short term wind speed forecasting using continuous cascade model* (2009), preprint.
- [51] M. K. Lauren, M. Menabde, and L. Austin, Boundary-Layer Meteorol. **100**, 263 (2001).
- [52] O. Chanal, B. Chabaud, B. Castaing, and B. Hebrat, Eur. Phys. J. B **17**, 309 (2000).
- [53] R. Baile, J. Muzy, and P. Poggi, *Intermittency of surface layer wind speed fluctuations in the meso-scale range: application to short term prediction* (2009), to appear in Proceedings of World Renewable Energy Congress, Bangkok, Thailand, 2009.